Journal of Materials Chemistry B

ROYAL SOCIETY OF CHEMISTRY

PAPER

View Article Online
View Journal

Cite this: DOI: 10.1039/c9tb02733e

Synthesis of spiropyran with methacrylate at the benzopyran moiety and control of the water repellency and cell adhesion of its polymer film†

Nobuo Murase, * Tsuyoshi Ando and Hiroharu Ajiro *

Received 2nd December 2019,
Accepted 20th January 2020

DOI: 10.1039/c9tb02733e

rsc.li/materials-b

Stimuli-responsive materials have been actively researched over the past few decades. Among such materials, spiropyran is one of the most attractive compounds because the structure and polarity of the material are dramatically changed after photo irradiation, unlike other materials. In this work, we designed and synthesized a spiropyran derivative (**SpMA**) with a methacryloyl group on the nitrobenzene ring of a spiropyran skeleton. The UV spectra of the newly synthesized **SpMA** showed the photo-isomerization of spiropyran. The maximum absorption wavelength (λ_{max}) of **SpMA** was 616 nm in *n*-hexane, a nonpolar solvent, although λ_{max} of **SpMA** was 532 nm in methanol, a polar protic solvent, which resulted in an 84 nm blue-shift. **SpMA** was successfully polymerized by ruthenium (Ru)-catalyzed living radical polymerization. Poly(**SpMA**) (PSpMA) was then spin-coated on a PET substrate in order to control the surface properties of water repellency and cell adhesion. The water repellency was decreased approximately 10° under UV irradiation, because of the polarity change of PSpMA caused by photo-isomerization from the spiropyran (SP) type to the merocyanine (MC) type. In addition, NIH3T3 cells were spread only on 6% of the surface of the PSpMA thin film after UV irradiation compared with no UV irradiation. The polarity change of PSpMA by photo-isomerization is also believed to be the reason for this behavior. As a result, we successfully synthesized a photo-controllable cell culture scaffold.

Introduction

Over the past few decades, many studies on stimuli-responsive materials have been conducted for a wide range of applications, such as for drug delivery,[1,2] controlled release systems,[3,4] biosensors,[5,6] and molecular machines[7] as actuators. Hitherto, light,[8–10] temperature,[11–14] pH,[15–17] electric fields[18] and magnetic fields,[19,20] *etc.* as external stimuli for stimuli-responsive materials have been widely studied. In particular, light is a very strong example of these stimuli because it is able to irradiate a local target in a short, controlled space of time without any chemical contamination. For this reason, many photo-responsive compounds have been used for stimuli-responsive materials. For instance, azobenzene[21,22] is the most widely used compound for *cis–trans* isomerization, as well as other compounds which have also been used for their specific mechanisms, such as spiropyran[23,24] for heterolytic cleavage, diarylethene[25] for electrocyclic reactions, and salicylideneaniline[26] for tautomerization. It is notable that the photo-isomerization of spiropyran dramatically changes not only the structure but also the polarity of the compound unlike many other photo-responsive compounds. Therefore, polymers with a spiropyran skeleton are very attractive as effective stimuli-responsive materials, such as for drug delivery and controlled release systems.[27–29]

M. Q. Zhu *et al.* reported on nanoparticle preparation with polymer bearing spiropyran–merocyanine dyes incorporated into their hydrophobic cavities, and they controlled the delivery of these nanoparticles into living cells by photo irradiation.[30] Interestingly, D. He *et al.* reported the fabrication of a soft interface of photo-controlled wettability and cell adhesion.[31] This was achieved by the synthesis of an amphiphilic diblock copolymer, consisting of a hydrophobic poly(methyl methacrylate) block with photo-responsive spiropyran molecules, as well as a hydrophilic PEG block. Moreover, A. Abdollahi *et al.* reported on functionalized stimuli-responsive latex particles, introducing spiropyran by semicontinuous emulsifier-free emulsion polymerization.[32] The prepared stimuli-responsive latexes were used as inks for writing on cellulosic paper. Y. Hao *et al.* reported a photo and thermo dual-responsive copolymer using spiropyran and *N*-isopropylacrylamide. They also confirmed the efficiency of cell capture and release using the dual-responsive copolymer.[33]

Division of Materials Science, Graduate School of Science and Technology, Nara Institute of Science and Technology, 8916-5 Takayama-cho, Ikoma, Nara 630-0192, Japan. E-mail: nmurase@ms.naist.jp, ajiro@ms.naist.jp

† Electronic supplementary information (ESI) available. See DOI: 10.1039/c9tb02733e

However, most of the previous studies used a spiropyran monomer, where a polymerizable methacryloyl group was introduced at the *N*-position on the indoline ring of a spiropyran skeleton. This molecular design results in a limited selection of co-monomers with small and less sterically hindered monomers, such as methyl methacrylate. Therefore, we decided to design a new spiropyran-based monomer, which could widen the range of possible applications from the view point of various polymerizations.

In this study, we designed a novel spiropyran derivative (**SpMA**) with a methacryloyl group on the nitrobenzene ring, in order to expand the range of possibilities for various polymerizations. The synthesized **SpMA** would actually use a living radical polymerization system by using a ruthenium (Ru) catalyst to demonstrate the possible precise polymerization. We also discuss spin-coated PSpMA films on a PET substrate in order to clarify the photo-responsive properties, through evaluation of the water repellency and cell adhesion.

Experimental section

Materials

Aluminum chloride ($AlCl_3$) (>98.0%), methacrylic acid (>99.0%), 25% ammonia solution (25.0–27.9%), silver nitrate (>99.8%), iodomethane (>95.0%), piperidine (>98.0%), sodium sulfate (>99.0%), 1,4-dioxane (>99.5%), trietylamine (>99.0%), sodium hydrogen carbonate (>99.5%), methyl ethyl ketone (MEK) (>98.0%), hexane (>96.0%), toluene (>99.0%), diethyl ether (>99.5%), chloroform (>99.0%), ethyl acetate (>99.0%), tetrahydrofuran (THF) (>99.5%), acetone (>99.0%), acetonitrile (>99.5%), *N*,*N*-dimethylformamide (DMF) (>99.5%), dimethyl sulfoxide (DMSO) (>99.0%), methanol (>99.8%), ethanol (>99.5%), and bovine serum albumin (BSA, pH 7.0) were obtained from FUJIFILM Wako Pure Chemical Corporation (Osaka, Japan). 5-Nitrosalicylaldehyde (>97.0%), chloromethyl methyl ether (CMME) (>95.0%), 2,3,3-trimethylindolenine (>97.0%) and *n*-tributylamine (*n*-Bu_3N) (>98.0%) were purchased from Tokyo Chemical Industry Co., Ltd (Tokyo, Japan). Methyl α-bromoisobutyrate (MBIB) (≥99.0%), sodium dodecyl sulfate (SDS) (>98.5%) and trypsin were purchased from Sigma-Aldrich Co., LLC. (USA). Chloro(indenyl)bis(triphenylphosphine)-ruthenium(II) (dichloromethane adduct): $Ru(Ind)Cl(PPh_3)_2$ was purchased from Santa Cruz Biotechnology, Inc. (USA). Ethylenediamine-*N*,*N*,*N*′,*N*′-tetraacetic acid (EDTA) (≥99.5%) was purchased from Dojindo Laboratories (Kumamoto, Japan). A protein assay bicinchoninate kit and calcein-AM (≥90.0%) were purchased from Nacalai Tesuque, Inc. (Kyoto, Japan). Dulbecco's modified Eagle's medium (DMEM) was purchased from Nissui Pharmaceutical Co., Ltd (Tokyo, Japan). Fetal calf serum (FCS) was purchased from HyClone Laboratories Inc. (USA). NIH3T3 cells (ATCC, CRL-1658) were obtained from Dainippon Sumitomo Pharma Co., Ltd (Osaka, Japan). PBS for cell adhesion tests was prepared with NaCl (8 g), KCl (0.2 g), KH_2PO_4 (0.2 g) and Na_2HPO_4 (1.15 g) in pure water (1 L). Organic solvents were used after drying by molecular sieves (FUJIFILM Wako Pure Chemical Corporation), and Milli-Q purified water was used (Gradient A10, Merck Millipore Corp, Germany).

Methods

Nuclear magnetic resonance (NMR) spectra were measured in $CDCl_3$ and *d*-DMSO using a 400 MHz spectrometer (JNM-ECP400, JEOL Ltd, Japan). The molecular weight was measured using DART-MS (JMS-Q1000TD, JEOL Ltd, Japan). Infrared spectroscopy (IR) spectra were measured using an FT-IR spectrometer (Spectrum One, PerkinElmer Inc., USA). Size exclusion chromatography (SEC) was performed in THF (2% triethylamine) at 1 mL min^{-1} at 40 °C on two columns (Shodex KF-806L, 8.0 mm I.D. × 30 cm × 2, Showa Denko K. K., Japan) connected in series with a pump (PU-2086 Plus), degasser (DG-2080-53), auto-sampler (AS-2055 Plus) (JASCO Corporation, Japan), column oven (L-7300), UV-vis detector (L-7420) and refractive index detector (L-7490) (Hitachi, Ltd, Japan). The relative molecular weight was calculated from a calibration curve of a PMMA standard sample (M_p = 875–1 916 000) in THF (2% triethylamine). UV spectra were measured by using a UV-vis spectrophotometer (V-550, Hitachi, Ltd, Japan). A 100 μM solution of **SpMA** was prepared using various solvents (hexane, toluene, diethyl ether, chloroform, ethyl acetate, THF, acetone, acetonitrile, DMF, DMSO, ethanol, and methanol). The UV absorption spectrum was measured under the following conditions (measurement wavelength: 250–750 nm, measurement rate: 2000 nm min^{-1}, slit width: 1 nm). Surface observations of PSpMA thin films coated on a PET substrate were carried out by scanning electron microscopy (SEM) (SU-6600, Hitachi, Ltd, Japan) at 50 k after the deposition of osmium for 5 s using vacuum deposition equipment (Neoc-ST, Meiwafosis Co., Ltd, Japan). Contact angle measurements were performed using a Drop Master (DM-501, Kyowa Interface Science Co., Ltd, Japan). The water contact angles were measured after 30 s by dropping water (2 μL) onto the surface. The captive bubble contact angles were measured after 30 s by dropping air (5 μL) onto the surface in water.

Synthesis of SpMA with a methacryloyl group on the nitrobenzene ring

SpMA was synthesized by the following procedure with reference to previous literature (Scheme 1).[34–36]

Synthesis of 3-chloromethyl-5-nitrosalicylaldehyde (2). In a baked 300 mL round-bottom flask, 5-nitrosalicylaldehyde (100 mmol, 16.7 g) was dissolved in dry CMME (100 mL) under argon. After cooling in an ice bath, $AlCl_3$ (200 mmol, 26.7 g) was gradually added and stirred for 1 h and then refluxed for 2 h. After the reaction, ice water (*ca.* 300 mL) was added, and the precipitated solid was washed with a large amount of water. The crude product was recrystallized from hot hexane. **2** was obtained as a yellow solid (yield: 78%).

^1H NMR ($CDCl_3$): δ 12.09 [1H, s, –OH], 10.02 [1H, d, –CHO], 8.55–8.58 [2H, m, φ], 4.72 [2H, s, $–CH_2–$], DART-MS: calcd for $C_8H_6ClNO_4$: 233.0 $[M + NH_4]^+$, found: 233.

Synthesis of silver methacrylate (4). In a 300 mL round-bottom flask, methacrylic acid (200 mmol, 16.9 mL) was added

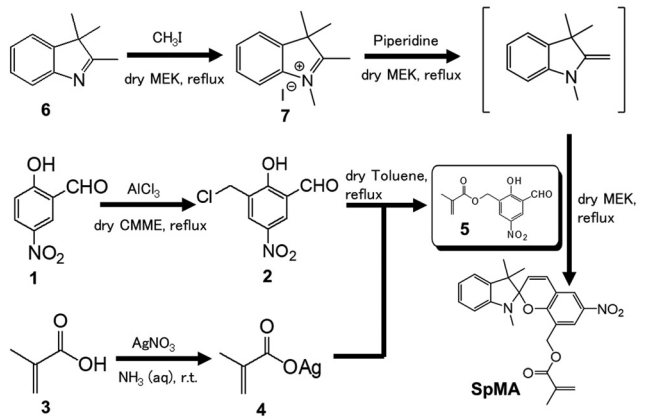

Scheme 1 Synthesis of **SpMA** with a methacryloyl group on the nitrobenzene ring.

and cooled in an ice bath. Then, 25% ammonia solution (20 mL) was gradually dropped into the flask. Next, silver nitrate (220 mmol, 37.4 g) in water (100 mL) was gradually added and stirred overnight at room temperature. The precipitated solid was purified by recrystallization in hot water. **4** was obtained as a silver-white solid (yield: 37%).

^{1}H NMR (*d*-DMSO): δ 5.77 and 5.25 [1H, each, s, $=CH_2$], 1.86 [3H, s, $-CH_3$].

Synthesis of 3-methacryloxymethyl-5-nitrosalicylaldehyde (5). In a baked 500 mL round-bottom flask, **2** (60 mmol, 12.9 g) and **4** (66 mmol, 12.7 g) were dissolved in dry toluene (400 mL) under argon and refluxed for 3 h. While the solution was hot, the precipitated solid was filtered through Celite®, and the solution was evaporated. The crude product was purified by silica gel column chromatography (silica gel 60, chloroform). **5** was obtained as a yellow-white solid (yield: 92%).

^{1}H NMR ($CDCl_3$): δ 11.96 [1H, s, –OH], 10.02 [2H, d, −CHO], 8.50–8.55 [2H, m, φ], 6.23 and 5.68 [1H, each, s, $=CH_2$], 5.34 [2H, s, $-CH_2-$], 2.01 [3H, s, $-CH_3$], DART-MS: calcd for $C_{12}H_{11}NO_6$: 266.1 $[M + H]^+$, found: 266.

Synthesis of 1,2,3,3-tetramethylindolenium iodide (7). In a baked 300 mL round-bottom flask, 2,3,3-trimethylindolenine (200 mmol, 32.1 mL) and iodomethane (220 mmol, 13.7 mL) were dissolved in MEK (100 mL) under argon and refluxed overnight. The reaction solution was evaporated and the obtained solid was washed with diethyl ether. The crude product was purified by recrystallization in ethanol. **7** was obtained as a white solid (yield: 82%).

^{1}H NMR (*d*-DMSO): δ 7.59–7.92 [4H, m, φ], 3.97 [3H, s, $N-CH_3$], 2.77 [3H, s, $N=C-CH_3$], 1.52 [6H, s, $-(CH_3)_2$], DART-MS: calcd for $C_{12}H_{16}N^+I^-$: 174.1 $[M]^+$, found: 174.

Synthesis of 8-methacryloyloxymethyl-1′,3′,3′-trimethyl-6-nitrospiro-[(2*H*)-1-benzopyran-2,2′-indoline] (SpMA). In a baked 500 mL round-bottom flask, **7** (50 mmol, 15.1 g) was dissolved in MEK (200 mL) under argon. Next, piperidine (55 mmol, 5.43 mL) was added and refluxed for 5 min to deiodinate. Then, **5** (50 mmol, 13.3 g) in MEK (100 mL) was added and refluxed for 8 h. The solvent was evaporated and ethyl acetate was added. The solution was washed with pure water three times and then brine. The organic layer was dried using sodium sulfate. The solid was filtrated and the solvent was evaporated. The crude product was purified by column chromatography (silica gel 60, ethyl acetate/hexane = 1 : 1 (v/v)). **SpMA** was obtained as a purple solid (yield: 74%).

^{1}H NMR ($CDCl_3$): δ 8.09 and 7.99 [2H, each, s, φ-NO_2], 6.85–7.27 [4H, m, φ], 6.52 [1H, d, $=CH-$], 6.06 and 5.58 [1H, each, s, methacryloyl = CH_2], 5.89 [1H, d, $-CH=$], 4.93–5.02 [2H, m, φ-CH_2–O], 2.71 [3H, N–CH_3], 1.90 [3H, s, methacryloyl-CH_3], 1.20 and 1.30 [3H, each, s, $-(CH_3)_2$] (Fig. S1 in the ESI†), DART-MS: calcd for $C_{24}H_{24}N_2O_5$: 421.2 $[M + H]^+$, found: 421, IR (cm^{-1}): 1727 [s, ν(C=O)], 1635 [w, ν(C=C)], 1608 [m, ν(C=C)], 1523 [s, ν(N–O)], 1484 [s, $\delta(CH_2)$], 1461 [s, ν(C=C)],1334 [s, ν(N–O)], 1313 [s, ν(C–N)], 743 [s, δ(CH)] (Fig. S2 in the ESI†).

Synthesis of the SpMA polymer (PSpMA). In a baked Schlenck flask, **SpMA** (0.8 mmol, 336 mg) and $Ru(Ind)Cl(PPh_3)_2$ (0.002 mmol, 1.72 mg) were dissolved in dry toluene (0.79 mL) under argon. Next, 1,4-dioxane (0.08 mL) diluted 10-fold with toluene and a 94 mM toluene solution of *n*-Bu_3N (0.04 mmol, 0.43 mL), and a 110 mM toluene solution of MBIB (0.04 mmol, 0.36 mL) were added to the flask under argon. The reaction solution was stirred at 80 °C after argon bubbling for approximately 10 min. After 168 h, the reaction was terminated by cooling in an ice bath. The conversion of **SpMA** was determined to be 69% based on the average reduction in the double bond peak (6.05 and 5.56 ppm) of the methacryloyl group, using 1,4-dioxane (3.69 ppm) as an internal standard for ^{1}H NMR. Subsequently, the quenched reaction solution was added dropwise to a large amount of methanol with stirring for purification of the obtained PSpMA by precipitation. The supernatant was removed, and the precipitate was dried *in vacuo*, producing PSpMA as a purple solid. SEC (PMMA) calibration in THF (2% triethylamine): (M_n = 3400, M_w/M_n = 3.56).

Spin-coating method of PSpMA on a PET substrate

A 0.1 wt% chloroform solution of PSpMA was prepared and the polymer solution (30 μL) was dropped onto a PET substrate (1 × 1 cm). A polymer thin film was formed by rotation at 2000 rpm for 60 s using a spin coater (MS-A100, Mikasa Co., Ltd, Japan). Then, the polymer thin film on the PET substrate was dried for 3 h *in vacuo*. This polymer thin film coated on a PET substrate was used in order to test the surface properties such as contact angle and cell adhesion.

Protein adsorption test

Protein (BSA) adsorption tests were performed for PSpMA thin films spin-coated on a PET substrate using a protein assay bicinchoninate kit and microplate reader (MTP-310Lab, Corona Electric Co., Ltd). First, each spin-coated film was incubated in BSA solution in PBS (1 mL, 4.5 mg mL^{-1}) for 3 h at room temperature. Next, the films were lightly washed with PBS three times, and immersed into saturated SDS solution in PBS (1 mL) for 3 h at room temperature to remove the absorbed protein from the thin film. The mixture of protein assay bicinchoninate kit solution (400 μL) and SDS solution (400 μL) containing the protein from the polymer thin film was incubated for 1 h at 37 °C.

Then, the UV absorbance of the mixture was measured with a microplate reader. The amount of absorbed protein was calculated using a calibration curve of the same protein.

Cell adhesion test

Dulbecco's modified Eagle medium (DMEM) (5.0 g) was dissolved in pure water (500 mL). Next, sodium hydrogen carbonate was added and stirred for 5 min. The DMEM solution was sterilized by a sterilization filter and then DMEM (10% FCS) was prepared by adding FCS (10 mL) to the DMEM solution (90 mL). NIH3T3 cells were cultivated in DMEM (10% FCS) (10 mL) in a T-type flask until approximately 80% confluency. After removing the supernatant liquid, the adhered cells were washed using sterile PBS (3 mL) and detached using 0.02% EDTA (1 mL) and 0.25% trypsin (1 mL). DMEM solution (3 mL) was then added and centrifuged at 1000 rpm for 5 min. The supernatant was removed by decantation and then DMEM solution was added and pipetting was performed. The cell number was counted using a hemocytometer and adjusted to 2.0×10^4 cells per cm^2 using DMEM solution. PSpMA spin-coated on a PET substrate was pasted in a 24-well cell culture plate. After that, pure water (1 mL) was poured into each well and incubated at room temperature overnight and at 37 °C in a 5% CO_2 incubator for 10 min. Half was covered with aluminum foil and the other half was irradiated with UV (365 nm) for 5 min. The pure water was then removed and the previously prepared NIH3T3 solution (1 mL) was dropped into each well of the cell culture plate. NIH3T3 cells were cultivated at 37 °C in a 5% CO_2 incubator for 3 h. The supernatant of the NIH3T3 suspension was removed and washed with PBS (1 mL). The adherent cells were stained with a little calcein-AM DMSO solution dissolved in PBS and observed with a fluorescence microscope after incubation at 37 °C in 5% CO_2 for approximately 5 min. The cell number was counted using ImageJ software (National Institutes of Health, USA).

Results and discussion

We measured the UV spectra of **SpMA** to confirm the photo-isomerization from the spiropyran (SP) type to the merocyanine (MC) type in chloroform. As a result, the absorbance at approximately 580 nm was increased by irradiating with UV at 365 nm for 2 min (Fig. 1a). The color of the spiropyran solution also changed from colorless to purple. After that, the spiropyran solution colored purple by UV light quickly returned to its original state after approximately 20 minutes under a fluorescent lamp (Fig. 1b) (All solution images and UV spectra of photo-isomerization are shown in Fig. S3 and S4 in the ESI.†)

We also measured the maximum absorption wavelength (λ_{max}) of the spiropyran solution on photo-isomerization to the MC type in various solvents. As shown in Fig. 2, as the relative permittivity of the solvent increased, λ_{max} shifted to the shorter wavelength side. In particular, when the relative permittivity did not exceed 5 (nonpolar solvent), λ_{max} decreased almost linearly. Furthermore, when the relative permittivity was between 5 and 50 (polar aprotic solvent), λ_{max} gradually decreased. On the other hand, λ_{max} dramatically decreased in the polar protic solvent (methanol and ethanol) compared with the polar aprotic solvent despite both having almost the same relative permittivity.

According to previous research,[37–40] it is known that λ_{max} is blue-shifted when a proton is added to an oxygen anion of the nitrobenzene ring under acidic conditions. Hence, we think that a proton was weakly bonded to an oxygen anion of the nitrobenzene ring, because the alcohol of a polar protic solvent is considered to be a very weak acid. As a result, λ_{max} is blue-shifted. These results imply that not only the relative permittivity of the solvent but also the proton donor greatly affect λ_{max} with photo-isomerization of spiropyran. These results also suggest photo-isomerization of PSpMA under UV irradiation.

We synthesized PSpMA by Ru-catalyzed living radical polymerization. The number average molecular weight (M_n) and M_w/M_n of the obtained polymer were 3400 and 3.56, respectively. The relatively broad molecular weight distribution could be due to the mixture of SP type and MC type spiropyran polymers, however, it is noteworthy that the novel monomer, **SpMA**, achieved homopolymerization in this study. The methacrylate polymer bearing spiropyran groups was obtained as a homopolymer, which would allow for a high density of spiropyran moieties on the material, leading to much more effective photo-responsivity. Moreover, the polymer structure could be specific due to the anion groups being closer than the cation groups along the main chain, when it is the MC type. Such reverse structures of electrostatic moieties would be

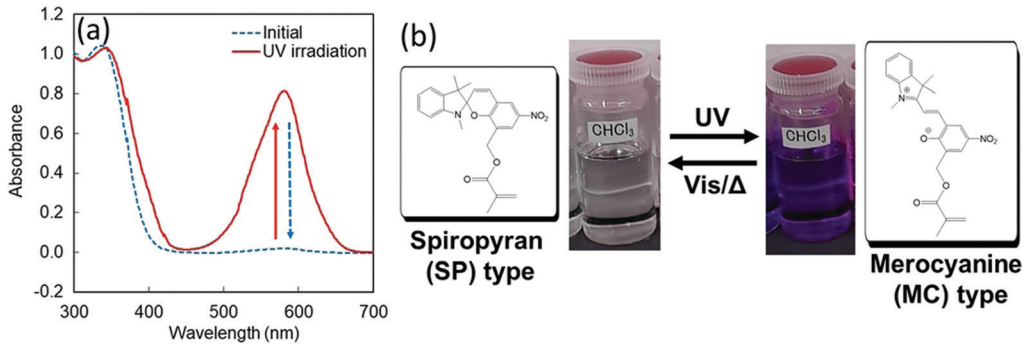

Fig. 1 UV spectra (a) and solution images (b) of photo-isomerization of synthesized **SpMA** in chloroform.

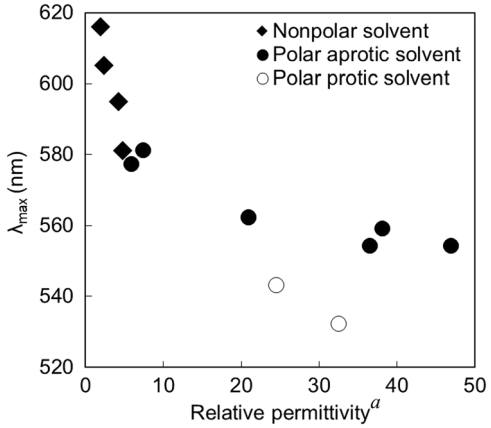

Fig. 2 λ_{max} *vs.* relative permittivity plots of the MC type of **SpMA** measured with various solvents. The relative permittivity of all solvents was obtained from the CRC Handbook of Chemistry and Physics (87th edition), and Vogel's Textbook of Practical Organic Chemistry (5th edition).

interesting from the view point of biocompatibility, such as the difference of sulfobetaine methacrylate[41] and methacryloyloxyethyl phosphorylcholine.[42] Therefore, the novel monomer could provide many possibilities in the field of photo-responsive materials, including various polymer architectures and electrostatic characteristics in the near future. First of all, we selected surface wettability and cell adhesion for evaluation in this study.

We measured the contact angle of water and captive bubbles on a PSpMA thin film spin-coated on a PET substrate to confirm photo-isomerization of **SpMA**. The water contact angle of PSpMA decreased approximately 10° from 87° in its initial state to 78° under UV irradiation (non-coated PET substrate: 74°) (Fig. 3).

In addition, the captive bubble contact angle of PSpMA increased approximately 10° from 111° in its initial state to 121° under UV irradiation (non-coated PET substrate: 112°) (Fig. 4). Generally, it is well known that the water repellency greatly depends on the surface free energy of the material and the finely rough structure of the surface.[43] Therefore, we observed the surface of the PSpMA thin film by SEM to eliminate the effect of rough surface-structure. Consequently, the surfaces of the PSpMA thin film were almost smooth both before and after UV irradiation (Fig. S5, ESI†).

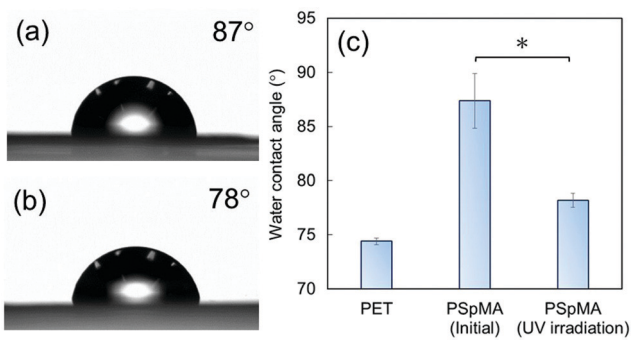

Fig. 3 Water repellency images of the initial state (a) and after UV irradiation (b), and the contact angle (c) of each substrate (*$p < 0.05$).

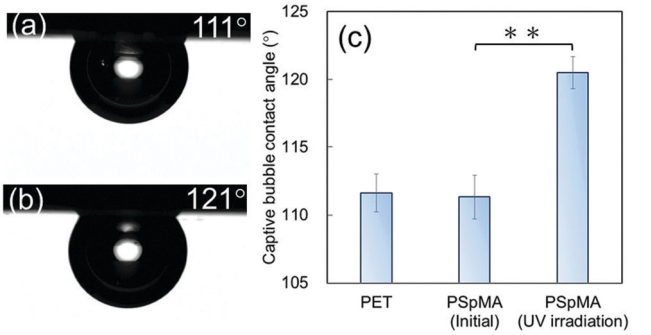

Fig. 4 Captive bubble images of the initial state (a) and after UV irradiation (b), and the contact angle (c) of each substrate (**$p < 0.01$).

Hence, we also think that these results might be due to the increase in polarity of PSpMA by the photo-isomerization from SP type to MC type under UV irradiation. These results, demonstrating that the hydrophilicity and hydrophobicity of the substrate can be photo-controlled, prompted us to use the material as a stimuli-responsive cell culture scaffold.

First, we carried out protein adsorption tests using a PSpMA thin film spin-coated on a PET substrate in its initial state and after UV irradiation, because cells combined with proteins on the film surface. Consequently, the amount of BSA adsorption was dramatically decreased on the PSpMA thin film after UV irradiation for 5 min. Namely, when PSpMA (initial) was normalized to 100, PSpMA (UV irradiation) was approximately 15% (Fig. S6, ESI†).

Based on these results, we carried out cell adhesion tests using a PSpMA thin film spin-coated on a PET substrate in its initial state and after UV irradiation in order to confirm its potential application to scaffold materials. NIH3T3 cells were spread across the entire surface of the substrate on an initial thin film of PSpMA (Fig. 5a). In contrast, few NIH3T3 cells were spread on a thin film of PSpMA cell-cultured after UV irradiation (Fig. 5b). Namely, when PSpMA (initial) was normalized to 100, PSpMA (UV irradiation) was approximately 6% (Fig. 5c). In addition, we calculated the aspect ratio of adhered cells from fluorescence microscope images in the initial state and after UV

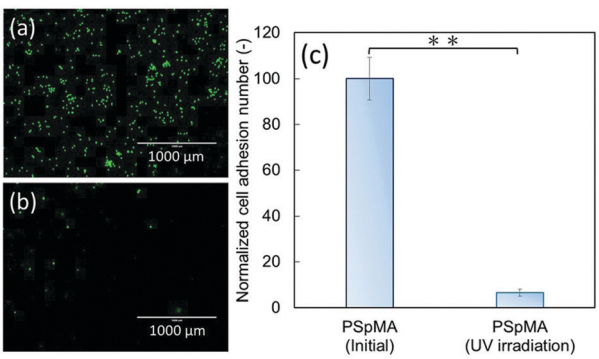

Fig. 5 Fluorescence microscope images of the cell adhesion test of PSpMA spin-coated on a PET substrate in the initial state (a) and after UV irradiation (b), and normalization of the cell adhesion number (c) (PSpMA (initial) = 100) (**$p < 0.01$).

irradiation to confirm the cell morphology. We found that cell spreading was slightly suppressed on the substrate after UV irradiation (the average aspect ratio of the initial state and after UV irradiation was approximately 1.88 and 1.35, respectively).

We hypothesize that this behavior is due to an increase of polarity from SP type to MC type caused by photo-isomerization of PSpMA. These results imply that it could be applied as a photo-controllable scaffold material for cell culture. This material may be usable as a recyclable cell culture scaffold by exposure to external stimuli.

Conclusions

We successfully designed and synthesized a spiropyran monomer (**SpMA**) with a methacryloyl group on the nitrobenzene ring of a spiropyran skeleton. We also homo-polymerized **SpMA** using Ru-catalyzed living radical polymerization. Subsequently, we measured the contact angle of water and captive bubbles in order to confirm photo-isomerization of the PSpMA thin film both under and not under UV irradiation. As a result, the water contact angle and captive bubble contact angle changed approximately 10° because of the polarity change caused by the photo-isomerization from SP type to MC type. The number of adhered NIH3T3 cells dramatically decreased on the substrate cell-cultured after UV irradiation. These results also imply that this is due to increased polarity by photo-isomerization of PSpMA. We successfully synthesized materials with photo-controllable surface properties using PSpMA. We think that these materials may be applied as recyclable cell culture scaffolds created by external stimuli, as well as various new polymer materials with copolymerization in the near future.

Conflicts of interest

There are no conflicts to declare.

References

1 D. Schmaljohann, Thermo- and pH-responsive polymers in drug delivery, *Adv. Drug Delivery Rev.*, 2006, **58**, 1655–1670.
2 S. Mura, J. Nicolas and P. Couvreur, Stimuli-responsive nanocarriers for drug delivery, *Nat. Mater.*, 2013, **12**, 991–1003.
3 E. S. Gil and S. M. Hudson, Stimuli-reponsive polymers and their bioconjugates, *Prog. Polym. Sci.*, 2004, **29**, 1173–1222.
4 S. Ganta, H. Devalapally, A. Shahiwala and M. Amiji, A review of stimuli-responsive nanocarriers for drug and gene delivery, *J. Controlled Release*, 2008, **126**, 187–204.
5 C. D. H. Alarcon, S. Pennadam and C. Alexander, Stimuli responsive polymers for biomedical applications, *Chem. Soc. Rev.*, 2005, **34**, 276–285.
6 M. Molina, M. Asadian-Birjand, J. Balach, J. Bergueiro, E. Miceli and M. Calderón, Stimuli-responsive nanogel composites and their application in nanomedicine, *Chem. Soc. Rev.*, 2015, **44**, 6161–6186.
7 M. A. C. Stuart, W. T. S. Huck, J. Genzer, M. Müller, C. Ober, M. Stamm, G. B. Sukhorukov, I. Szleifer, V. V. Tsukruk, M. Urban, F. Winnik, S. Zauscher, I. Luzinov and S. Minko, Emerging applications of stimuli-responsive polymer materials, *Nat. Mater.*, 2010, **9**, 101–113.
8 F. Ercole, T. P. Davis and R. A. Evans, Photo-responsive systems and biomaterials: photochromic polymers, light-triggered self-assembly, surface modification, fluorescence modulation and beyond, *Polym. Chem.*, 2010, **1**, 37–54.
9 J. F. Gohy and Y. Zhao, Photo-responsive block copolymer micelles: design and behavior, *Chem. Soc. Rev.*, 2013, **42**, 7117–7129.
10 O. Bertrand and J. F. Gohy, Photo-responsive polymers: synthesis and applications, *Polym. Chem.*, 2017, **8**, 52–73.
11 E. S. Ron and L. E. Bromberg, Temperature-responsive gels and thermogelling polymer matrices for protein and peptide delivery, *Adv. Drug Delivery Rev.*, 1998, **31**, 197–221.
12 N. A. Cortez-Lemus and A. Licea-Claverie, Poly(*N*-vinylcaprolactam), a comprehensive review on a thermoresponsive polymer becoming popular, *Prog. Polym. Sci.*, 2016, **53**, 1–51.
13 S. Strandman and X. X. Zhu, Thermo-responsive block copolymers with multiple phase transition temperatures in aqueous solution, *Prog. Polym. Sci.*, 2015, **42**, 154–176.
14 Y. J. Kim and Y. T. Matsunaga, Thermo-responsive polymers and their application as smart biomaterials, *J. Mater. Chem. B*, 2017, **5**, 4307–4321.
15 G. Kocak, C. Tuncer and V. Butun, pH-Responsive polymers, *Polym. Chem.*, 2017, **8**, 144–176.
16 Y. Ohya, Temperature-responsive biodegradable injectable polymer systems with conveniently controllable properties, *Polym. J.*, 2019, **51**, 997–1005.
17 M. Kanamala, W. R. Wilson, M. M. Yang, B. D. Palmer and Z. M. Wu, Mechanisms and biomaterials in pH-responsive tumour targeted drug delivery: A review, *Biomaterials*, 2016, **85**, 152–167.
18 J. Thévenot, H. Oliveira, O. Sandre and S. Lecommandoux, Magnetic responsive polymer composite materials, *Chem. Soc. Rev.*, 2013, **42**, 7099–7116.
19 N. N. Reddy, Y. M. Mohan, K. Varaprasad, S. Ravindra, P. A. Joy and K. M. Raju, Magnetic and electric responsive hydrogel-magnetic nanocomposites for drug-delivery application, *J. Appl. Polym.*, 2011, **122**, 1364–1375.
20 K. Sutani, I. Kaetsu and K. Uchida, The synthesis and the electric-responsiveness of hydrogels entrapping natural polyelectrolyte, *Radiat. Phys. Chem.*, 2001, **61**, 49–54.
21 P. Weis, W. Tian and S. Wu, Photoinduced liquefaction of azobenzene-containing polymers, *Chem. – Eur. J.*, 2018, **24**, 6494–6505.
22 C. Fedele, P. A. Netti and S. Cavalli, Azobenzene-based polymers: emerging applications as cell culture platforms, *Biomater. Sci.*, 2018, **6**, 990–995.
23 B. I. Lpe, S. Mahima and K. G. Thomas, Light-induced modulation of self-assembly on spiropyran-capped gold nanoparticles: A potential system for the controlled release of amino acid derivatives, *J. Am. Chem. Soc.*, 2003, **125**, 7174–7175.

24 M. Q. Zhu, L. Y. Zhu, J. J. Han, W. W. Wu, J. K. Hurst and A. D. Q. Li, Spiropyran-based photochromic polymer nanoparticles with optically switchable luminescence, *J. Am. Chem. Soc.*, 2006, **128**, 4303–4309.
25 R. Kashihara, M. Morimoto, S. Ito, H. Miyasaka and M. Irie, Fluorescence photoswitching of a diarylethene by irradiation with single-wavelength visible light, *J. Am. Chem. Soc.*, 2017, **139**, 16498–16501.
26 P. Xue, R. Lu, G. Chen, Y. Zhang, H. Nomoto, M. Takafuji and H. Ihara, Functional organogel based on a salicylideneaniline derivative with enhanced fluorescence emission and photochromism, *Chem. – Eur. J.*, 2007, **13**, 8231–8239.
27 R. Klajn, Spiropyran-based dynamic materials, *Chem. Soc. Rev.*, 2014, **43**, 148–184.
28 V. I. Minkin, Photo-, thermo-, solvato-, and electrochromic spiroheterocyclic compounds, *Chem. Rev.*, 2004, **104**, 2751–2776.
29 F. J. Jiang, S. Chen, Z. Q. Cao and G. J. Wang, A photo, temperature, and pH responsive spiropyran-functionalized polymer: Synthesis, self-assembly and controlled release, *Polymer*, 2016, **83**, 85–91.
30 M. Q. Zhu, L. Zhu, J. J. Han, W. Wu, J. K. Hurst and A. D. Q. Li, Spiropyran-based photochromic polymer nanoparticles with optically switchable luminescence, *J. Am. Chem. Soc.*, 2006, **128**, 4303–4309.
31 D. He, Y. Arisaka, K. Masuda, M. Yamamoto and N. Takeda, A photoresponsive soft interface reversibly controls wettability and cell adhesion by conformational changes in a spiropyran-conjugated amphiphilic block copolymer, *Acta Biomater.*, 2017, **51**, 101–111.
32 A. Abdollahi, K. Sahandi-Zangabad and H. Roghani-Mamaqani, Rewritable anticounterfeiting polymer inks based on functionalized stimuli-responsive latex particles containing spiropyran photoswitches: Reversible photopatterning and security marking, *ACS Appl. Mater. Interfaces*, 2018, **10**, 39279–39292.
33 Y. Hao, H. Liu, G. Li, H. Cui, L. Jiang and S. Wang, Photo and thermo dual-responsive copolymer surfaces for efficient cell capture and release, *ChemPhysChem*, 2018, **19**, 2107–2112.
34 M. Hirano, K. Osakada, H. Nohira and A. Miyashita, Crystal and solution structures of photochromic spirobenzothiopyran. first full characterization of the meta-stable colored species, *J. Org. Chem.*, 2002, **67**, 533–540.
35 N. Murase, T. Mukawa, H. Sunayama and T. Takeuchi, Molecularly imprinted polymers bearing spiropyran-based photoresponsive binding sites capable of photo-triggered switching for molecular recognition activity, *J. Polym. Sci., Part B: Polym. Phys.*, 2016, **54**, 1637–1644.
36 T. Khalil, A. Alharbi, C. Baum and Y. Liao, Facile synthesis and photoactivity of merocyanine-photoacid polymers, *Macromol. Rapid Commun.*, 2018, **39**, 1800319.
37 A. Doron, E. Katz, G. L. Tao and I. Willner, Photochemically-, chemically-, and pH-controlled electrochemistry at functionalized spiropyran monolayer electrodes, *Langmuir*, 1997, **13**, 1783–1790.
38 A. Garcia, M. Marquez, T. Cai, R. Rosario, Z. B. Hu, D. Gust, M. Hayes, S. A. Vail and C. D. Park, Photo-, thermally, and pH-responsive microgels, *Langmuir*, 2007, **23**, 224–229.
39 A. Abdollahi, A. Mouraki, M. H. Sharifian and A. R. Mahdavian, Photochromic properties of stimuli-responsive cellulosic papers modified byspiropyran-acrylic copolymer in reusable pH-sensors, *Carbohydr. Polym.*, 2018, **200**, 583–594.
40 K. Sumaru, T. Takagi, T. Satoh and T. Kanamori, Photo- and thermoresponsive dehydration of spiropyran-functionalized polymer regulated by molecular recognition, *Macromol. Rapid Commun.*, 2018, **39**, 1700234.
41 R. Lalani and L. Liu, Electrospun zwitterionic poly(sulfobetaine methacrylate) for nonadherent, superabsorbent, and antimicrobial wound dressing applications, *Biomacromolecules*, 2012, **13**, 1853–1863.
42 T. Ueda, H. Oshida, K. Kurita, K. Ishihara and N. Nakabayashi, Preparation of 2-methacryloyloxyethyl phosphorylcholine copolymers with alkyl methacrylates and their blood compatibility, *Polym. J.*, 1992, **24**, 1259–1269.
43 N. Murase, K. Terada, T. Ando, S. Shibutani, Y. Tanaka and T. Kawabe, Water repellency of bottlebrush polymers consisting of monomer units with a long alkyl chain synthesized by Ru-catalyzed living radical polymerization, *ACS Appl. Polym. Mater.*, 2019, **1**, 3422–3431.